Journal of Coastal Research	17	1	146–161	West Palm Beach, Florida	Winter 2001

Phytoplankton Variability in Summer in the Northwestern Mediterranean: Modelling of the Wind and Freshwater Impacts

Christel Pinazo†, Patrick Marsaleix‡, Bertrand Millet†, Claude Estournel‡, Véronique Kondrachoff‡, and Raoul Véhil‡

†Centre d'Océanologie de Marseille
Université de la Méditerranée
Campus de Luminy
F-13288 Marseille Cedex 9, France

‡Laboratoire d'Aérologie
Université Paul Sabatier
Observatoire Midi-Pyrénées
14, avenue Edouard Belin
31400 Toulouse, France

ABSTRACT

PINAZO, C.; MARSALEIX, P.; MILLET, B.; ESTOURNEL, C.; KONDRACHOFF, V., and VÉHIL, R., 2001. Phytoplankton variability in summer in the northwestern Mediterranean: modelling of the wind and freshwater impacts. *Journal of Coastal Research*, 17(1), 146–161. West Palm Beach (Florida), ISSN 0749-0208.

A coupling between a 3-D mesoscale hydrodynamic model and a biogeochemical model was performed in the northwestern Mediterranean to reproduce the major processes of carbon and nitrogen cycles involved in the new production of phytoplankton biomass. The study was focused on simulating the real conditions of the EURHOGLI campaign, performed in summer in the Gulf of Lions (June–July 1983). Results of the coupled model showed the high variability of the Rhône river plume position and the associated phytoplankton biomass. The validation of the model was in good accordance with field measurements and CZCS and AVHRR remote sensing pictures available at the period considered. In addition, results showed that the phytoplankton biomass induced by freshwater nutrients was strongly controlled by the variability of the local wind conditions. The model, performed with representative forcing conditions, allowed to better understand the representative phytoplankton features that prevails in summer in the Gulf of Lions, where both strong winds and freshwater runoffs interact.

ADDITIONAL INDEX WORDS: *Numerical model, physical and biogeochemical coupling, phytoplankton biomass, freshwater supply, northwestern Mediterranean.*

INTRODUCTION

The Gulf of Lions is the area, located in the northwestern Mediterranean, with a wide continental shelf of about 15000 km^2. This coastal zone is influenced by the Rhône river, the most important river of the western Mediterranean, with sufficient flow and nutrient inputs to make the Gulf of Lions the most productive zone of the western Mediterranean. This area is also one of the most windy region of the Mediterranean, bordered by relatively high mountains separated by valleys, which induce typical northwestern wind conditions (LEFÈVRE et al., 1997). The local wind regime is dominated by two opposite wind directions: the northwestern wind, which is the most frequent (54%), and the southeastern wind (18%). The western wind (7%) represents a secondary sector occurring mostly in summer (ASCENSIO *et al.*, 1977).

Many field campaigns performed in the Gulf of Lions emphasized the major source of nutrients constituted by the Rhône river discharges: HYDROMEDE I, Mediterranean Hydrology (COSTE and MINAS, 1967); EURHOGLI, EUtrophication from the RHOne in the Gulf of Lions (MINAS and MINAS, 1990); DYPOL and PANACHE, variability of the exchanges between land and ocean, focused on the turbid layer (LOCHET, 1991); the EROS campaigns (MINAS and MINAS, 1992; LEFÈVRE *et al.*, 1995).

The present work aimed at giving a new insight into the time-space dynamics of the phytoplankton biomass relating to the environmental conditions prevailing at meso-scale in the plume and the dilution area of the Rhône river in the Gulf of Lions, and interacting with the local wind regime. We considered phytoplankton dynamics through the variability of a biomass expressed in chlorophyll a, that led to replace our study at the period of the year when the phytoplankton composition was low diversified. The summer period in the Gulf of Marseille is featured by the presence of only four phytoplankton species, two diatoms and two dinoflagellates (LEFÈVRE *et al.*, 1997). Thus, the EURHOGLI campaign, conducted in June and July 1983, and focused on the study of the Rhône's impact on phytoplankton biomass (FREIJE, 1985), was very well adapted to our study expressed in undifferenciated phytoplankton biomass.

In addition, the EURHOGLI sampling design was well adapted to the initialization and the validation of a modelling experiment, because wide spatial extension and two legs in a fortnight. Moreover, the variability of the Rhône's plume shape was observed from a set of Coastal Zone Color Scanner images (CZCS), available during the same EURHOGLI sampling period (DEMARCQ, 1985).

98096 received 27 March 1998; accepted in revision 27 January 2000.

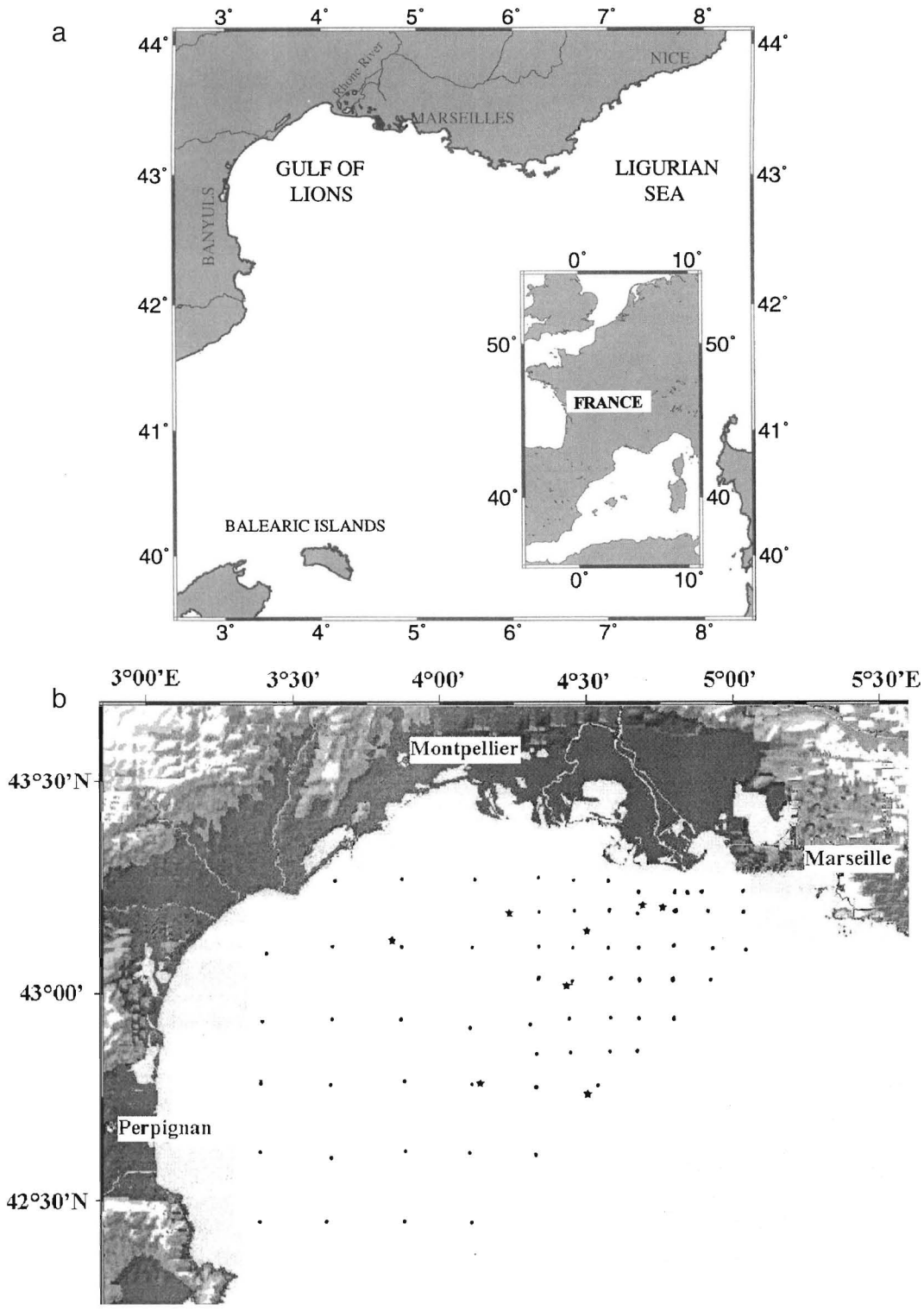

Figure 1. Sampling design of the two legs of the EURHOGLI campaign. A: general map; B: first leg 22 th of June–5th of July 1983 ; C: second leg 8th – 17th of July 1983. Stations of hydrology (points) ; stations of production (stars).

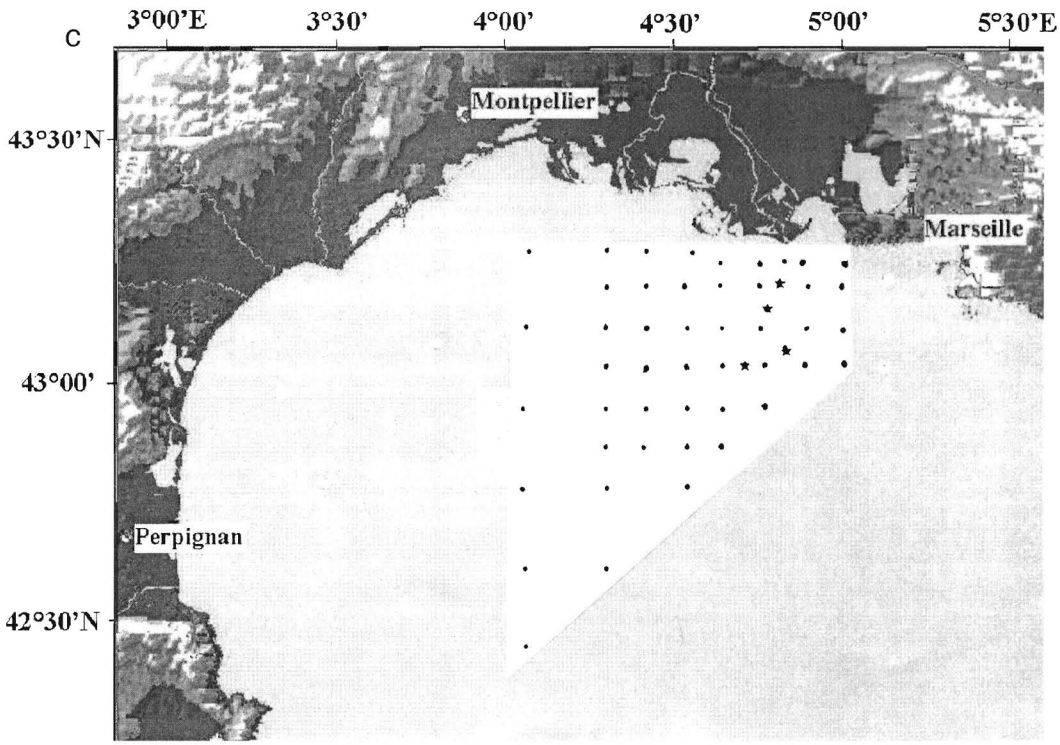

Figure 1. Continued.

The Rhône river plume appeared as a relatively high productive area compared with the surrounding oligotrophic waters of the Gulf of Lions (El Sayed *et al.*, 1994). The plume was featured by a high variability in space and time, according to the local meteorological conditions. Therefore, a numerical model coupling physical and biological processes was required to deal with the high level of non linear and complex interactions that occurred within this coastal ecosystem. Many recent studies were performed in various coastal sites in using coupled models, which therefore presented drastic differences concerning their different time-space resolution and biological description. Indeed, some models focused on complex biological algorithms with relative coarse time-space resolutions: 1DV with 7 biogeochemical variables as Kühn and Radach (1997) and 2DH with 8 variables as Van den Berg *et al.* (1997). Other models focused on an accurate spatial resolution with simple biological description: 1DV with 4 biogeochemical variables as Doney *et al.* (1996); 2DV with 3 variables as Chen *et al.* (1997), and 3D with 3 variables as Civitarese *et al.* (1996) or Fennel and Neumann (1996). Particularly in the Gulf of Lions, Tusseau *et al.* (1998) suggested an annual nutrient budget computed from a coupled model featured by a 3D grid of 11x11 km horizontal mesh, vertical z coordinates from 6m to 140m and a 1-hour time step, with an elaborated biogeochemical description through the computation of 13 state variables. We took a particular attention to propose, in our study, a compromise to make our coupled model easily involved in a 3D- fine-grid, and sufficiently adapted to the complexity of the biogeochemical cycles, at mesoscale, in the Gulf of Lions. Thus, we developed a coupled physical-biogeochemical model with a 3D fine resolution grid of a 4×4 km horizontal mesh, a 20 vertical sigma levels until a maximum depth of 500 m, a short time step of 20 mn. In addition, the biogeochemical model structure chosen was a quasi-PZND (Phytoplankton-Zooplankton-Nutrient-Detritus) with equations of 7 state variables focused on

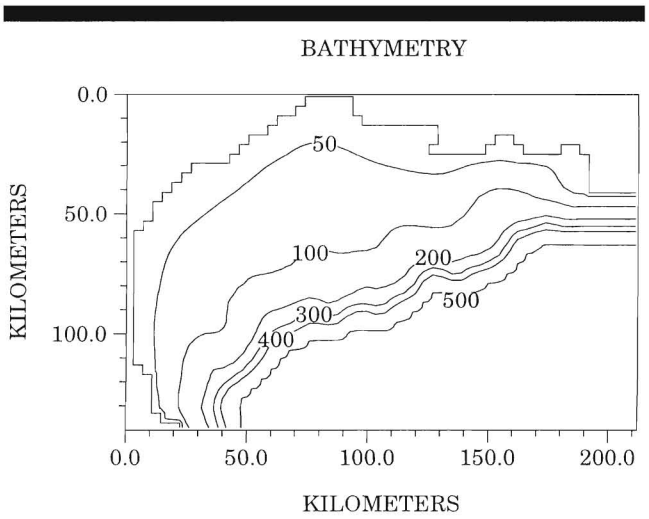

Figure 2. Bathymetry of the Gulf of Lions (isolines in meters) and morphology of the coast line considered in the numerical model.

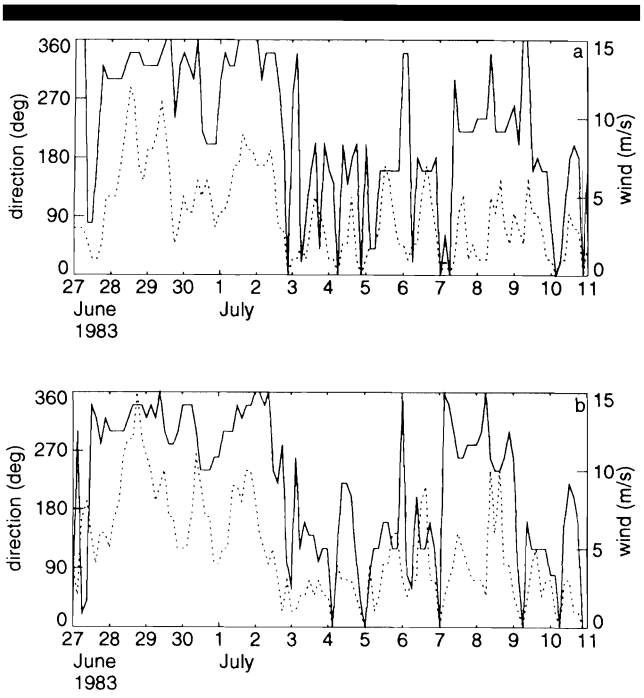

Figure 3. Time series of wind intensities (dashed line) and directions (solid line) respectively recorded at the Tour du Valat (a) and Cap Couronne (b) stations.

the major processes of carbon and nitrogen cycles involved in the new production of phytoplankton biomass.

Simulations were performed to represent both the biological dynamics of sources and sinks, and the advection and diffusion of the biogeochemical components according to the frequent changes of environmental conditions. Model parameters were cautiously not numerically adapted, but provided mostly from experiments performed in vitro and in northwestern Mediterranean sites, in order to avoid, as noticed by FASHAM (1995), the adoption of a particular set of computed parameters that would not correspond to the « inherent variability of the observations ». To compute a realistic EURHOGLI environment, unstationnary simulations were run by real observations of wind, meteorological forcing and freshwater runoff.

The validation of the coupled model was conducted from observed salinity, nitrate and chlorophyll concentrations, which was consistant with the study of a coastal ecosystem under freshwater influence. In addition, the high variability of the plume shape was validated by available CZCS and AVHRR remote sensing pictures that provided, contrary to field measurements, synoptic mappings of the area.

MATERIAL AND METHODS

Hydrodynamic Model

Model Description

The hydrodynamic model used, *Symphonie,* was the same as in PINAZO *et al.* (1996a). Details on the model can be found in JOHNS *et al.* (1991) and accordingly, only its recent developments and its essential features are presented here.

The model was a 3D primitive equation, sigma coordinate, circulation model. The prognostic variables considered were the free surface elevation, the two components of the horizontal velocity, the temperature, the salinity and the turbulence kinetic energy (TKE). The hydrostatic equilibrium and the Boussinesq approximation were included in the formulation of the governing equations. The local density was related to the local temperature and salinity of the water by a linearized equation of state. The turbulence closure, at the order 1.5, was based on the parametrization described in GASPAR *et al.* (1990). According to MELLOR and BLUMBERG (1985), an isosigma formulation of the horizontal diffusion was chosen, with a horizontal mixing coefficient of 20 $m^2 \cdot s^{-1}$.

Equations were solved on a three dimensional (3-D) "staggered" C grid (ARAKAWA and SUAREZ, 1983). A leap-frog differencing scheme associated with an Asselin (1972) filter was used for the time stepping of 6 mn. In order to avoid the computation load that the solution of the full set of the 3-D equations characterizing the fast moving surface wave would entail, a mode-splitting approach (BLUMBERG and MELLOR, 1987) was used to calculate separatly the transport and the elevation of the surface from the 3-D structure.

Boundary Conditions

At the surface, the turbulent flux of momentum was calculated using the wind speed, according to WU (1980). The surface turbulent flux of temperature was deduced from the atmospheric net heat flux given by the sum of sensible, latent and net infrared flux respectively parametrized following WU (1992a, 1992b) and QUENEY (1974). The surface salt flux was determined from the evaporation rate (BLUMBERG and MELLOR, 1987), which was itself deduced from the latent heat flux. The surface turbulent kinetic energy value, depending on wind stress, was calculated according to CANIAUX *et al.* (1993).

At the open boundaries, the free surface elevation was calculated by a radiation equation (ORLANSKI, 1976). At the eastern boundary, the model was forced by the geostrophic current associated with the inflowing large scale circulation.

The Rhône river system was represented by a 2DV model without taking into account the velocity and differencing terms in the direction perpendicular to the river bed. This approximation is justified by the fact that the baroclinic Rossby radius is larger than the estuary width (about 1 km). The transition between the river model and the oceanic model, which satisfied the continuity of the sea surface elevation and the volume fluxes across the river mouth section, was an adaptation of JOHNS and ALI (1980) to our three dimensional case.

Initial Conditions

The EURHOGLI campaign made it possible to obtain numerous measurements of temperature, salinity, dissolved oxygen, phosphate, nitrate, nitrite and silicate over the continental shelf of the Gulf of Lions and especially in the dilution area of the Rhône river. During this campaign, a roughly

Table 1. *Equations and processes of the biogeochemical model.*

Phytoplankton biomass expressed in carbon:

$$\frac{\partial C_B}{\partial t} + u\frac{\partial C_B}{\partial x} + v\frac{\partial C_B}{\partial y} + (w + w_B)\left(\frac{\partial C_B}{\partial z}\right) = \mu \cdot C_B - G \cdot C_B - m \cdot C_B - r \cdot C_B + \frac{\partial}{\partial z}\left(K\frac{\partial C_B}{\partial z}\right)$$

advection | sink | growth | grazing | death | respiration | vert. diff.

Phytoplankton biomass expressed in nitrogen:

$$\frac{\partial N_B}{\partial t} + u\frac{\partial N_B}{\partial x} + v\frac{\partial N_B}{\partial y} + (w + w_B)\left(\frac{\partial N_B}{\partial z}\right) = up \cdot C_B - G \cdot N_B - m \cdot N_B + \frac{\partial}{\partial z}\left(K\frac{\partial N_B}{\partial z}\right)$$

advection | sink | uptake | grazing | death | vert. diff.

Particulate detritic carbon:

$$\frac{\partial C_D}{\partial t} + u\frac{\partial C_D}{\partial x} + v\frac{\partial C_D}{\partial y} + (w + w_D)\left(\frac{\partial C_D}{\partial z}\right) = f \cdot G \cdot C_B + m \cdot C_B - \text{minc} \cdot C_D + \frac{\partial}{\partial z}\left(K\frac{\partial C_D}{\partial z}\right)$$

advection | sink | faeces | death | mineralization | vert. diff.

Particulate detritic nitrogen:

$$\frac{\partial N_D}{\partial t} + u\frac{\partial N_D}{\partial x} + v\frac{\partial N_D}{\partial y} + (w + w_D)\left(\frac{\partial N_D}{\partial z}\right) = f \cdot G \cdot N_B + m \cdot N_B - \text{minn} \cdot N_D + \frac{\partial}{\partial z}\left(K\frac{\partial N_D}{\partial z}\right)$$

advection | sink | faeces | death | mineralization | vert. diff.

Dissolved ammonia:

$$\frac{\partial N_H}{\partial t} + u\frac{\partial N_H}{\partial x} + v\frac{\partial N_H}{\partial y} + w\frac{\partial N_H}{\partial z} = -upN_H \cdot C_B + e \cdot G \cdot N_B + \text{minn} \cdot N_D - nit \cdot N_H + \frac{\partial}{\partial z}\left(K\frac{\partial N_H}{\partial z}\right)$$

advection | uptake | excretion | mineralization | nitrification | vert. diff.

Dissolved nitrate:

$$\frac{\partial N_o}{\partial t} + u\frac{\partial N_o}{\partial x} + v\frac{\partial N_o}{\partial y} + w\frac{\partial N_o}{\partial z} = -upN_o \cdot C_B + nit \cdot N_H + \frac{\partial}{\partial z}\left(K\frac{\partial N_o}{\partial z}\right)$$

advection | uptake | nitrification | vert. diff.

Dissolved oxygen:

$$\frac{\partial O}{\partial t} + u\frac{\partial O}{\partial x} + v\frac{\partial O}{\partial y} + w\frac{\partial O}{\partial z} = \mu \cdot C_B - r \cdot C_B - \text{minc} \cdot C_D - 2nit \cdot N_H + 2upN_o \cdot C_B + \frac{\partial}{\partial z}\left(K\frac{\partial C_B}{\partial z}\right)$$

advection | growth | respiration | mineralization | nitrification | reduction | vert. diff.

Table 2. *Parameters of the biogeochemical model.*

parameter	description	value	unit
w_B	phytoplankton sinking rate	7.5.10 $^{-6}$ (Bienfang, 1982)	m.s $^{-1}$
w_D	detritus sinking rate	10 $^{-1}$ (Andersen and Nival, 1988)	m.s $^{-1}$
$\mu_{max}(T) = a.e^{b.T}$	maximum growth rate	a = 9.851134.10 $^{-6}$ and b = 0.063321 (Eppley, 1972)	s $^{-1}$
α	initial slope of the curve $L_{fPAR} = f(PAR)$	12.5.10 $^{-3}$ (Steele, 1962)	$(J.m^{-2}.s^{-1})^{-1}$
G	grazing rate	1.157407.10 $^{-6}$ (Cloern, 1991; Skogen *et al.*, 1995)	s $^{-1}$
m	death rate	4.629630.10 $^{-7}$ (Andersen, Nival and Harris, 1996)	s $^{-1}$
r	respiration rate	1.157407.10 $^{-6}$ (Cloern, 1991; Druet and Zielinski, 1994)	s $^{-1}$
$(upN_o)_{max}$	maximum uptake rate of nitrate	4.5.10 $^{-6}$ (Caperon and Meyer, 1972)	$mmol(N).(mmol(C))^{-1}.s^{-1}$
K_{N_o}	half-saturation constant for nitrate	0.30 (Caperon and Meyer, 1972)	$mmol(N).m^{-3}$
$(upN_H)_{max}$	maximum uptake rate of ammonia	1.1.10 $^{-5}$ (Caperon and Meyer, 1972)	$mmol(N).(mmol(C))^{-1}.s^{-1}$
K_{N_H}	half-saturation constant for ammonia	0.20 (Caperon and Meyer, 1972)	$mmol(N).m^{-3}$
f	faeces fraction	0.3 (Andersen, Nival and Harris, 1987)	dimensionless
minc	detritic carbon mineralization rate	3.472222.10 $^{-7}$ (Peterson and Festa, 1984)	s $^{-1}$
minn	detritic nitrogen mineralization rate	1.041667.10 $^{-6}$ (Andersen and Nival, 1988)	s $^{-1}$
$e = k_e(1 - f)$	excretion rate	k_e = 0.5 (Tett, 1990a)	dimensionless
$(nit_{max})_0$	maximum nitrification rate at zero ° Celsius	2.899519.10 $^{-6}$ (Tett, 1990a)	s $^{-1}$
K_{O_2}	half-saturation constant for oxygene	30 (Tett, 1990a)	$mmol(O_2).m^{-3}$

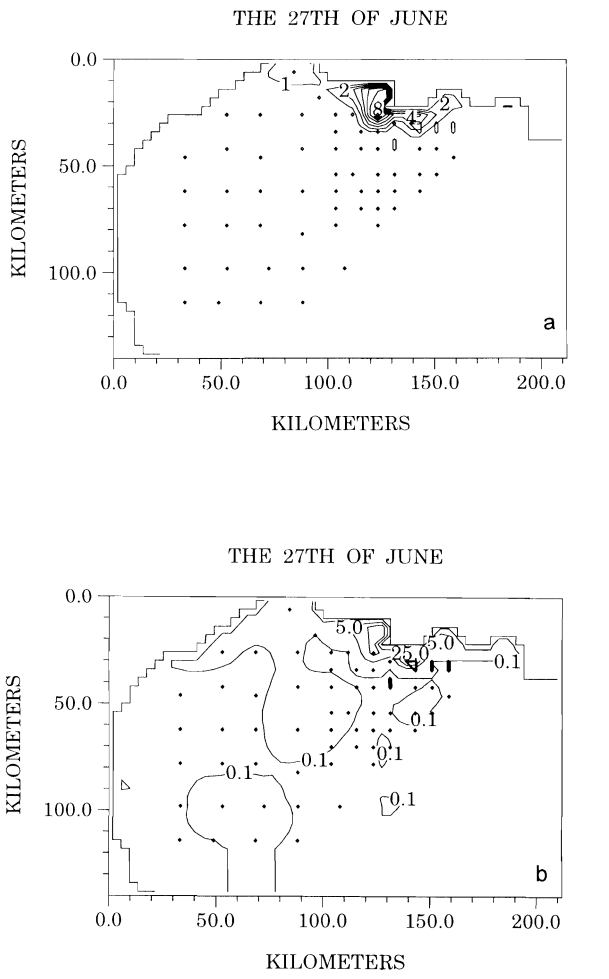

Figure 4. Initial conditions at the sea surface computed from measurements located at the sampling stations (points), of chlorophyll concentrations in mg·m^{-3} (a), of nitrate concentrations in mmol·m^{-3} (b).

150 km× 100 km domain was investigated between 3°30E 5°00E and 42°30N 43°30N. The first part of the campaign, performed between the 23th and the 27th of June 1983, consisted of 65 successive stations of hydrology, while during the second part of the campaign, 46 stations of hydrology were visited between the 8th and the 10th of July 1983 (represented by points on Figure 1). Between the two legs of the campaign and after the second leg, primary production measurements (represented by stars on Figure 1) were achieved in addition of the classical hydrological and biogeochemical observations previously mentioned.

The spatial extension of the model corresponded roughly to the domain covered by the EURHOGLI campaign. The model grid was constituted of 20 levels on the vertical, with a horizontal resolution of 4 km. As in PINAZO *et al.* (1996a), the maximum depth was restricted to 500m according to considerations on the accuracy of phytoplankton biomass computation near the surface (Figure 2).

The atmospheric fluxes at the surface were calculated, using the wind recorded every 3 hours by the meteorological stations located along the coast (Cap Béar, Perpignan, Sète, Montpellier, Tour du Valat, Cap Couronne and Marseille), the atmospheric pressure, the temperature, the humidity of air given every 6 hours by the meteorological model of the ECMWF[1], and the sea surface temperature calculated by the oceanic model. The solar flux was function of the mean latitude and longitude of the studied area and the astronomic parameters.

The physical simulation involved a first stage whose purpose was to provide initial conditions for the coupled physical biogeochemical simulation. This initialization stage was performed so that the resulting temperature and salinity fields were as close as possible to the observed situation corresponding to the first leg of EURHOGLI. This stage was accomplished in the following way: the model was forced by the general circulation and by the discharge of the Rhône freshwaters while vertical profiles of temperature and salinity were relaxed toward the measurements obtained at the first 65 stations.

The meso-scale general circulation in the Gulf of Lions is characterised by an eastern inflowing current identified as the Liguro-Provençal-Catalan (LPC) or as the Northern Current (MILLOT, 1990). The density associated with this current was forced at the eastern boundary using the most eastern hydrological stations (47, 48, 58, 59, 64, 65). The eastern forcing current consisted of geostrophic velocities, computed from the density section previously described, with a level of no motion at 500m. The resulting current, mainly concentrated in the upper 300 m, was roughly 40 km wide and represented a 0.5 Sv flux. These characteristics were in rather good agreement with the summer observations of the main branch of the LPC current off Marseille reported by CONAN and MILLOT (1995) and were consistent with the summer observations of the LPC in the Ligurian Sea performed by ALBÉROLA *et al.* (1995). The Rhône river outflow measured at the station of Beaucaire, located at 70 km upstream from the mouth, was fixed at 1500 m^3·s^{-1}, which corresponded to the mean discharge during EURHOGLI. The relaxation of temperature and salinity toward the field measurements was achieved through a nudging procedure in which, the weight of the forcing solution was determined through a time scale of 24 hours.

Conditions of Simulation

The simulation began on the 27th of June, the first leg's last day, and ended on the 10th of July, the second leg's last day. The atmospheric fluxes were computed (as for initial conditions) at each time step and grid point from meteorological data interpolated in space and time.

The wind measured at the meteorological stations of Tour du Valat and Cap Couronne (Figure 3), close to the Rhône river mouth, was a strong northwestern wind between the 27th of June and the 2nd of July with a short break during the 30th of June. Since the 3rd of July, the wind regime corresponded to a sea breeze cycle, which stopped during the night and was roughly orientated southern during the day: a

[1]European Center for Medium-range Weather Forecasts

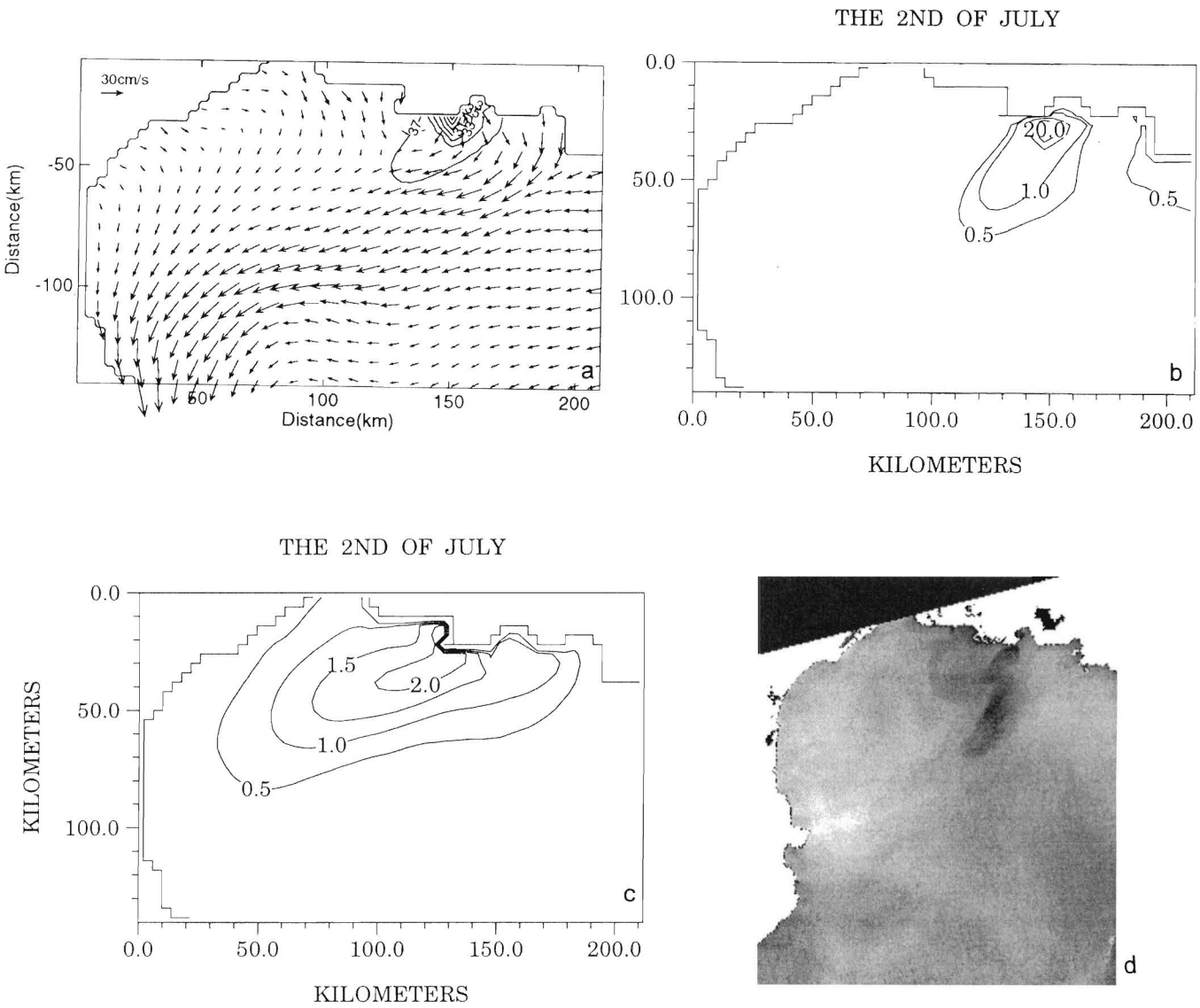

Figure 5. Results computed on the 2nd of July 1983, after five days of simulation: surface salinity and currents (a), chlorophyll concentrations in $mg \cdot m^{-3}$ (b) and nitrate concentrations in $mmol \cdot m^{-3}$ (c). CZCS image showing the distribution of chlorophyll on the 2nd of July (d).

weak to moderate alternative southwestern and southeastern wind until the 6th and then, a moderate southwestern wind blew until the 8th of July, turned southeastern the 9th, before blowing southwestern the 10th. Offshore wind events being characterized by the formation of strong inertial oscillations (MILLOT and CRÉPON, 1981), currents presented here were averaged over an inertial period of about 17.5 hours.

The Rhône river discharge was interpolated from the observations given every 24 hours at the station of Beaucaire. During the EURHOGLI campaign the river flow was low (between 1300 to 1900 $m^3 \cdot s^{-1}$), which were values consistent with the interannual monthly averaged flows observed during the 1967–83 period (1700 $m^3 \cdot s^{-1}$ for June and 1400 $m^3 \cdot s^{-1}$ for July) (FREIJE, 1985).

Biogeochemical Model

Model Description

A coupled model, with 7 state biogeochemical variables, was built to describe the nitrogen and carbon cycles involved in the production of phytoplankton biomass. The model structure chosen was a quasi-PZND (Phytoplankton-Zooplankton-Nutrient-Detritus) taking into account zooplankton only as a theoretical population with undifferentiated and static (no migration) plankters.

The seven state variables considered are: the phytoplankton expressed in carbon and nitrogen concentrations, the detritus expressed in carbon and nitrogen concentrations, the dissolved nutrients expressed in ammonia and nitrate and

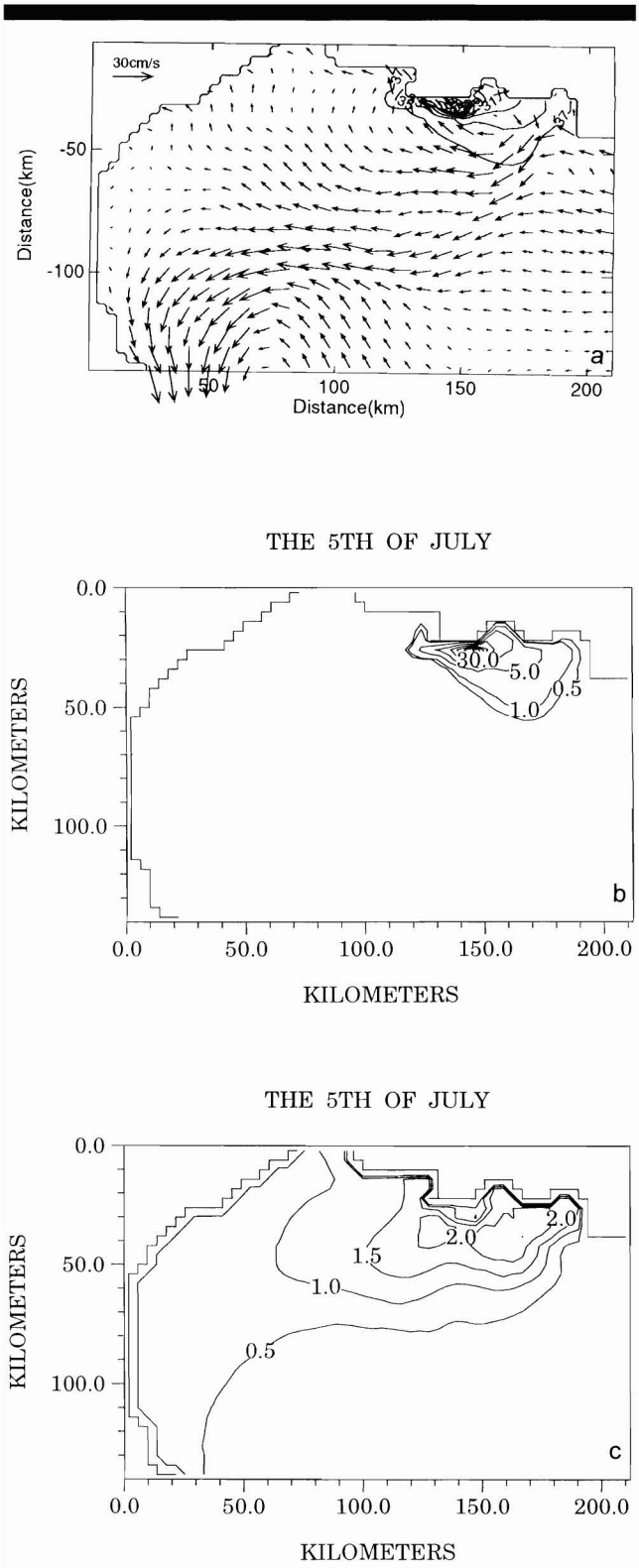

Figure 6. Results computed on the 5th of July 1983, after eight days of simulation: surface salinity and currents (a), chlorophyll concentrations in mg·m $^{-3}$ (b) and nitrate concentrations in mmol·m $^{-3}$ (c).

the dissolved oxygen concentration. Table I, presents the biogeochemical equations and processes considered in the model: the photosynthetic growth, the respiration and the death of phytoplankton, the grazing, the excretion and the feaces of zooplankton, the mineralization of detritic matter, the nitrification, the uptake and the nitrate reduction by phytoplankton.

The growth rate was a function of a maximum growth rate depending on the temperature (EPPLEY, 1972), a light limiting factor taking into account the photoinhibition (STEELE, 1962) and a nutrient limiting factor according to the cell-quota (CAPERON and MEYER, 1972a; TETT, 1987). A particularity of the biogeochemical model was the cell-quota, which allowed the determination of the nutritional state of the cells through the comparison of the phytoplankton nitrogen:carbon ratio (= cell-quota) with the Redfield ratio. Consequently, the nutritional state of the phytoplankton cells was taken into consideration to calculate both the growth rate through the nutrient limiting factor, and the uptake rate which didn't depend only on the nutrients concentration of the water. The nitrification rate was a function of the temperature with a $Q_{10} = 2$ for bacteria, and of the concentration of dissolved oxygen. The other parameters such as grazing pressure, respiration, mortality and mineralization rates were still considered as constant values. The sinking rates, different for phytoplankton cells and detritic matter, were directly introduced into the vertical advection term. The zooplankton was not considered as a state variable but merely as a constant fraction of the phytoplankton biomass. This theoretical biomass directly drove forcing functions of grazing and excretion of ammonium and feaces. The carbon dioxide was considered unlimited in the water column.

The parameters are presented in Table II, especially selected from experiments in laboratories (STEELE,1962; CAPERON and MEYER, 1972a and b; EPPLEY, 1972) and field measurements in northwestern Mediterranean sites (BIENFANG, 1982; ANDERSEN *et al.*, 1987; ANDERSEN and NIVAL, 1988). The description of the formulation of the biogeochemical processes was presented more in details in PINAZO *et al.* (1996a).

The calculation of the photosynthetic process required the forcing of the biogeochemical model by the photosynthetically available radiation (PAR), which was calculated from meteorological data of maximum total solar irradiance. A periodic function reproduced from I_{0max}, the maximum solar irradiance at midday, the diurnal variation of the solar irradiance I_0 just above the sea surface with the formulation described by PINAZO *et al.* (1996a). According the formulation of TETT (1990b), the fraction of the solar irradiance, which was photosynthetically available, represented only 0.46 of the total solar energy flux. In addition, there was a fraction of 0.05 of the energy lost by reflection at the sea surface and to take into account the more rapid attenuation of polychromatic light near the sea surface, only 0.37 of the radiation was available at the surface, as follows:

$$PAR_0 = (0.46)\cdot(0.95)\cdot(0.37)I_0 \text{ expressed in } (J\cdot m^{-2}\cdot s^{-1})$$

An exponential function calculated the vertical light attenuation with a specific algorithm, added to take into consideration the self-shading of phytoplankton:

Table 3. *Results of the model validation.*

Date	Number of Measurements Used for Interpolation	Salinity (psu)	Nitrate mmole.m $^{-3}$	CHL a mg.m $^{-3}$
8th of July	13	Figures 8a and 8d Computation with consistent concentrations within the plume and slightly surestimated westwards	Figures 8b and 8e Computation with consistent plume shape and slightly underestimated concentrations	Figures 8c and 8f Computation with wider plume, slightly higher concentrations and located more eastwards than observations
9th of July	18	Figures 9a and 9d Computation with consistent plume shape and location, and slightly surestimated concentrations	Figures 9b and 9e Computation with weaker plume extention and lower concentrations than observations	Figures 9c and 9f Computation with consistent concentrations and located more eastwards than observations
10th of July	14	Figures 10a and 10d Computation with more restricted plume	Figures 10b and 10e Computation with very low values as observations	Figures 10c and 10f Computation with slightly higher concentrations

$$PAR = PAR_0 \cdot e^{-k \cdot z} \text{ expressed in } (\mu E \cdot m^{-2} \cdot s^{-1})$$

with the extinction factor:

$$k = k_0 + A_{Chl} \cdot R_{Chl\text{-}N} \cdot N_B \text{ expressed in } (m^{-1})$$

k_0 is the extinction factor of the sea water expressed in (m^{-1})

A_{Chl} is the absorption factor of the Chlorophyll expressed in $(m^2 \cdot (mg \cdot Chl)^{-1})$

$R_{Chl\text{-}N}$ is the Chlorophyll/Nitrogen ratio expressed in $(mg \cdot Chl \cdot (mmol \cdot N)^{-1})$

N_B is the nitrogen concentration of the phytoplankton cells expressed in $(mmol \cdot N \cdot (m)^{-3})$

Coupling Description

The coupling task consisted in forcing the advective-diffusive scheme of the biogeochemical model by physical parameters, such as velocities and vertical eddy diffusivities. The biogeochemical algorithm allowing the calculation of the growth rate of the phytoplankton, was also forced by the temperature previously calculated by the hydrodynamic model and updated in the biogeochemical model with the same procedure. In order to facilitate the coupling between the two models, the advective-diffusive numerical scheme used in the biogeochemical model was the same as the one used in the physical model, with the same spatial grid. At each time step of twenty minutes, and for each state variable, the biogeochemical model first computed the biological dynamics of the variable in a specific subroutine and then, its physical dynamics in an advective -diffusive subroutine, forced by the physical parameters (temperatures, velocities and coefficients of vertical eddy diffusivity) previous calculated by the 3D hydrodynamic model.

Initial Conditions

The initial conditions for the biogeochemical model were determined from the first leg of the EURHOGLI campaign. The simulation of the biogeochemical model started from the 27th of June, the last day of the first leg. The chlorophyll, nitrate and dissolved oxygen initial concentrations were horizontally and vertically calculated from the measured data. Figure 4a presents the initial chlorophyll concentrations at the sea surface, calculated from the measured data at 65 stations, by a kriging model with a spherical spatial distribution which preserved original data. The biomass concentrations were relatively high and reached the value of 9.0 mg·m $^{-3}$ in the west side of the Rhône river mouth. In depth, a typical vertical profile of chlorophyll concentrations, determined from the measured data at 13 stations, was applied. Figure 4b presents the initial nitrate concentrations at the sea surface, calculated from the measured data at 65 stations. The nitrate concentrations were moderate and reached the value of 30.0 mmol·m $^{-3}$ in the plume. In depth, the nitrate concentrations were also calculated from the measured data. The dissolved ammonia concentrations were initialized with the constant value of 0.4 mmol·m $^{-3}$ and the detritus concentrations were initialized at zero.

The initial concentrations in the Rhône river were determined from the measured values during the EURHOGLI campaign (FREIJE, 1985) and the seasonal values given by SOTO *et al.* (1993). The initial concentrations in the Rhône river were 50.0 mmol·m $^{-3}$ for dissolved nitrate, 7.0 ml·l $^{-1}$ for dissolved oxygen, 3.0 mmol·m $^{-3}$ for ammonia, 1500.0 mmol·m $^{-3}$ for detritic carbon and 90.0 mmol·m $^{-3}$ for detritic nitrogen. A zero initial chlorophyll concentration was also assumed to represent marine phytoplankton in freshwater.

RESULTS

First, the physical and biogeochemical results obtained during the simulation (between the 27th of June and the 10th of July 1983) are presented to show the variability of the plume shape according to meteorological conditions. Second, the numerous measurements performed between the 8th and the 10th were compared with the computed results in order to attempt an horizontal validation of the models.

Wind Influence on the Rhône River Plume

The results showed mainly the variability of the plume shape, associated with the wind forcing because in the case

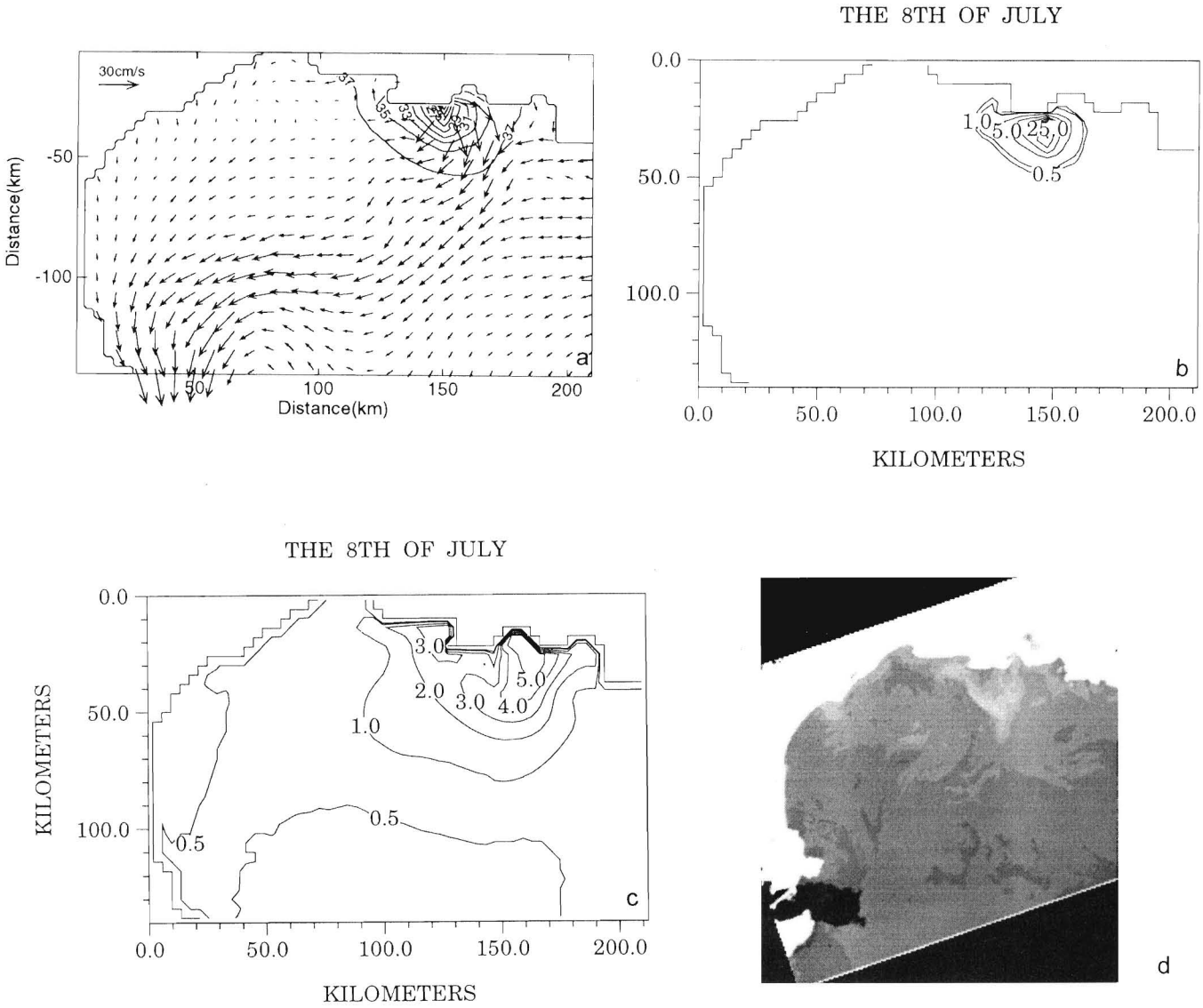

Figure 7. Results computed on the 8th of July 1983, after eleven days of simulation: surface salinity and currents (a), chlorophyll concentrations in mg·m^{-3} (b) and nitrate concentrations in mmol·m^{-3} (c). Thermal satellite observation (AVHRR) of the Gulf of Lions on the 8th of July 1983. The lighter shades indicate the warmer waters (d).

of weak Rhône river flow (less than 2000 m^3·s^{-1}), the orientation and the extension of the plume are driven by meteorological conditions (DEMARCQ, 1985).

Unfortunately, the very few measurements performed from the 27th of June until the 7th of July (only 13 stations during 11 days), and the lack of vertical investigation did not allow, nor the surface validation, neither the vertical distribution of the concentrations simulated during this period. However, the different plume shapes calculated by the model were compared with the classification of wind dependent plume shapes suggested by DEMARCQ and WALD (1984), and with some CZCS and AVHRR remote sensing pictures taken during the campaign.

The 2nd of July

Figure 5a presents the surface salinity and the surface currents calculated by the hydrodynamical model on the 2nd of July, after 5 days of simulation. The computed plume, after a strong northwestern wind period, was clearly orientated offshore and southwestwards. Figure 5b shows the surface nitrate concentrations that presented the same pattern than the sea surface salinity, with a plume extending offshore southwestwards and with lower concentrations compared with initial conditions (maximum concentrations of 22.4 mmol·m^{-3} near the mouth). In addition, a concentration of 0.5 mmol·m^{-3} of nitrate, close to the coast of Marseille,

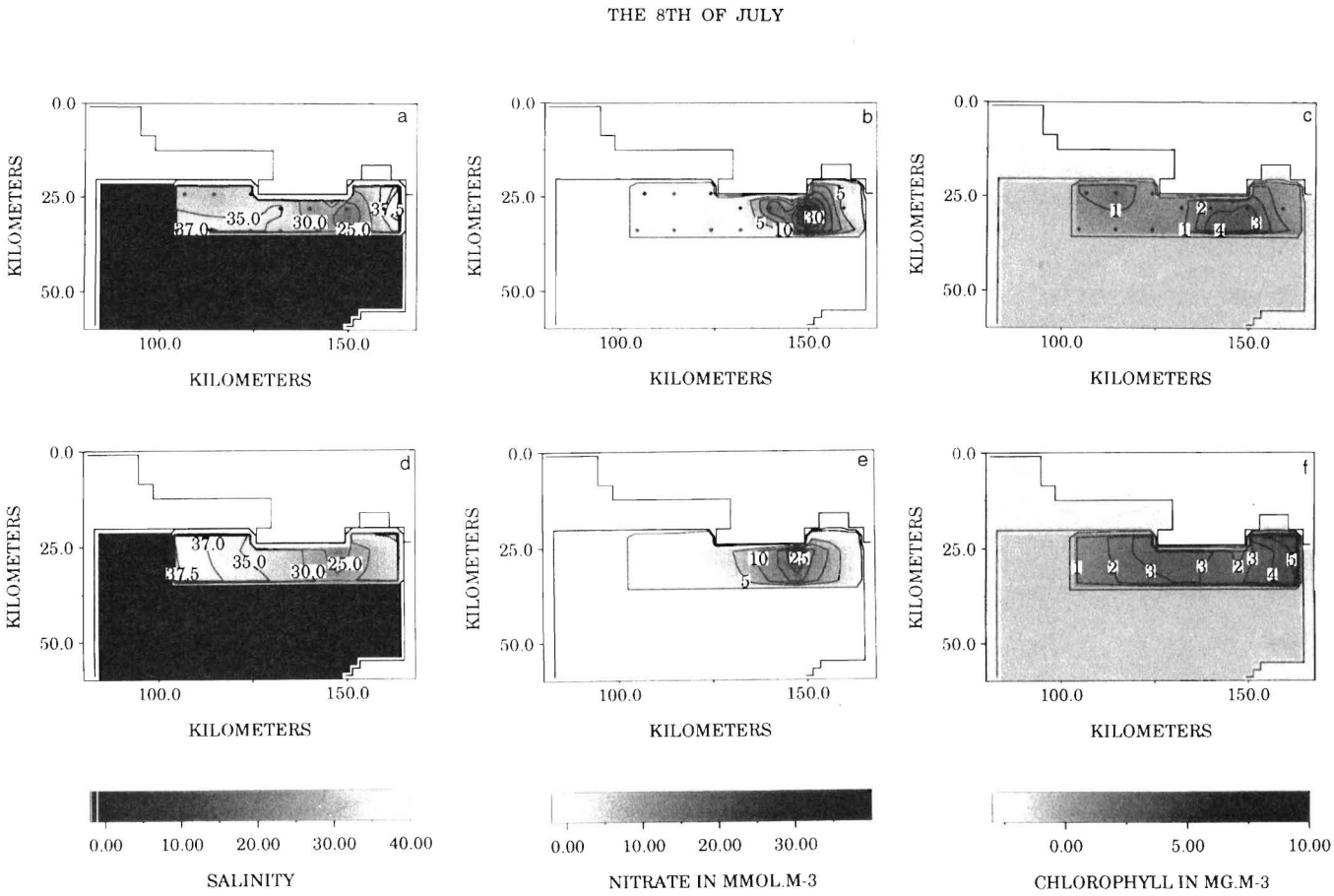

Figure 8. Comparative diagram of respectively measured salinity (a), nitrate (b), chlorophyll (c) and computed salinity (d), nitrate (e), chlorophyll (f), on the 8th July 1983.

showed an upwelling induced by the strong northwestern wind. The chlorophyll concentrations were lower than the initial conditions (maximum value of 2.2 $mg \cdot m^{-3}$ of chlorophyll) with a southwestwards chlorophyll plume extension (Figure5c). This southwestwards orientation of the plume computed by the model, was consistent with the CZCS remote sensing picture of the 2nd of July (Figure 5d).

The 5th of July

Since the 3rd of July, the wind turned and blew alternately from southwest and southeast. Figure 6a presents the surface salinity and the surface currents calculated by the hydrodynamical model on the 5th of July, after 8 days of simulation. The southern wind narrowed the plume and pushed it against the coast. Surface nitrate concentrations (Figure 6b) presented a pool expanding mainly along the shore and entering in the Gulf of Fos, which was consistent with the plume shape observed with the salinity during this southern wind period. The nitrate concentrations increased with a maximum value of 32.6 $mmol \cdot m^{-3}$ close to the Rhône's mouth. Figure 6c, which presents the surface chlorophyll concentrations, shows that the Rhône river nutrient supply, associated with a southern wind, induced a patch that extended northeastwards, with a slow increase of concentrations (maximum value of 2.5 $mg \cdot m^{-3}$ of chlorophyll) compared with previous northwestern conditions.

The 8th of July

Figure 7a presents the surface salinity and the surface currents calculated by the hydrodynamical model on the 8th of July, after 11 days of simulation with a weak to moderate western wind, which blew since the 7th of July and promoted a low extension of the plume southwards. Surface nitrate concentrations (Figure 7b) presented a similar plume extending southwards. The nitrate concentrations decreased with a maximum value of 30 $mmol \cdot m^{-3}$ close to the Rhône's mouth. Figure 7c, which presents the surface chlorophyll concentrations, shows an increase of phytoplankton biomass with a maximum value of 5.7 $mg \cdot m^{-3}$ of chlorophyll in the Gulf of Fos. The extension of high chlorophyll concentrations along the coast was very wide: from the Espiguette westward until the Gulf of Fos and the Gulf of Marseille eastward. This wide extension was consistent with the wide chlorophyll plume observed on the CZCS remote sensing picture of the 8th of July

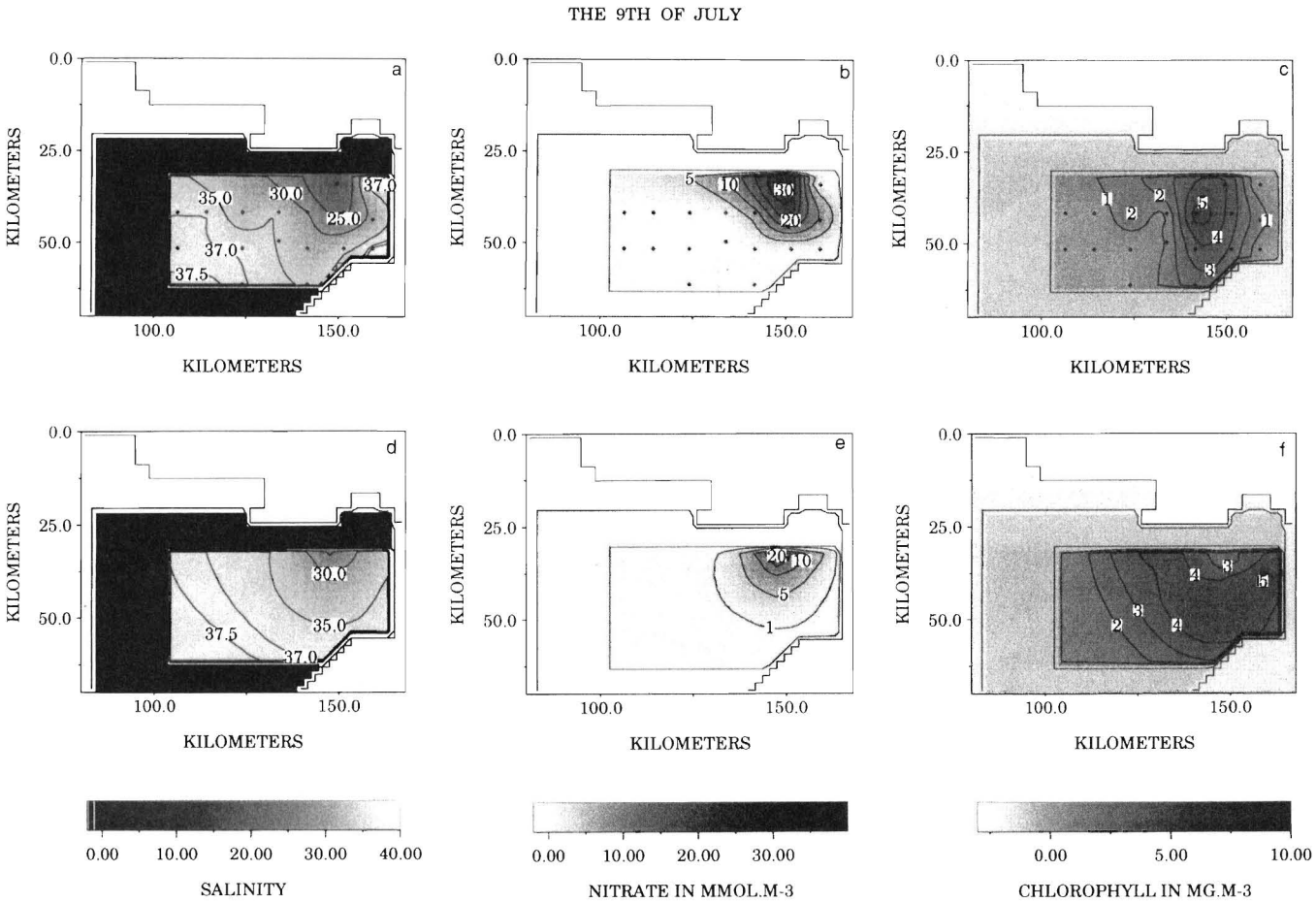

Figure 9. Comparative diagram of respectively measured salinity (a), nitrate (b), chlorophyll (c) and computed salinity (d), nitrate (e), chlorophyll (f), on the 9th July 1983.

(DEMARCQ, 1985). Figure 7d shows the AVHRR remote sensing picture of the 8th of July, which emphasizes a thermic spatial structure quite similar to the chlorophyll patch.

Results of Validation

The field measurements obtained during the second leg of EURHOGLI, were compared with the results of the simulation during the same period, in the same area close to the Rhône river mouth. The main problem encountered to compare the measurements and the models results, was the respective time and space scales of measures and calculations. The area of validation was investigated during a 3 day period, from the 8th until the 10th of July, whereas the models gave results at every grid points, every 20 minutes. It was difficult to choose model results for the validation, all the more as the wind changed during this period. To avoid this problem, we chose to represent models results in the same way as field measurements. For each day, from the 8th to the 10th of July, we compared in the same area the interpolation of surface measured values with the daily-average surface computed values. Results are synthesized in Table III.

DISCUSSION

Validation of the Plume Shape According to Wind Impact

It is important to note that the Rhône river inflow during the campaign remained lower than 2000 $m^3 \cdot s^{-1}$, which means, following DEMARCQ (1985), that the Rhône's plume was very influenced by wind conditions with a relatively short time of response of about six hours. Our computed results, forced by realistic wind conditions, confirm the strong influence of the wind in driving the different plume shapes.

First, on the 2nd of July, the northwestern wind induced oceanic circulation was orientated southwestwards, as expected under such wind conditions by DEMARCQ and WALD (1984) or BECKERS (1991).

Second, on the 5th of July, the southern wind narrowed the plume and pushed it nearshore, in the same way as observed by DEMARCQ and WALD (1984). However, it is noteworthy that these authors observed a plume that did not extend so much to the east, because forced only by southeastern wind. In our case, the alternation between the southeastern and

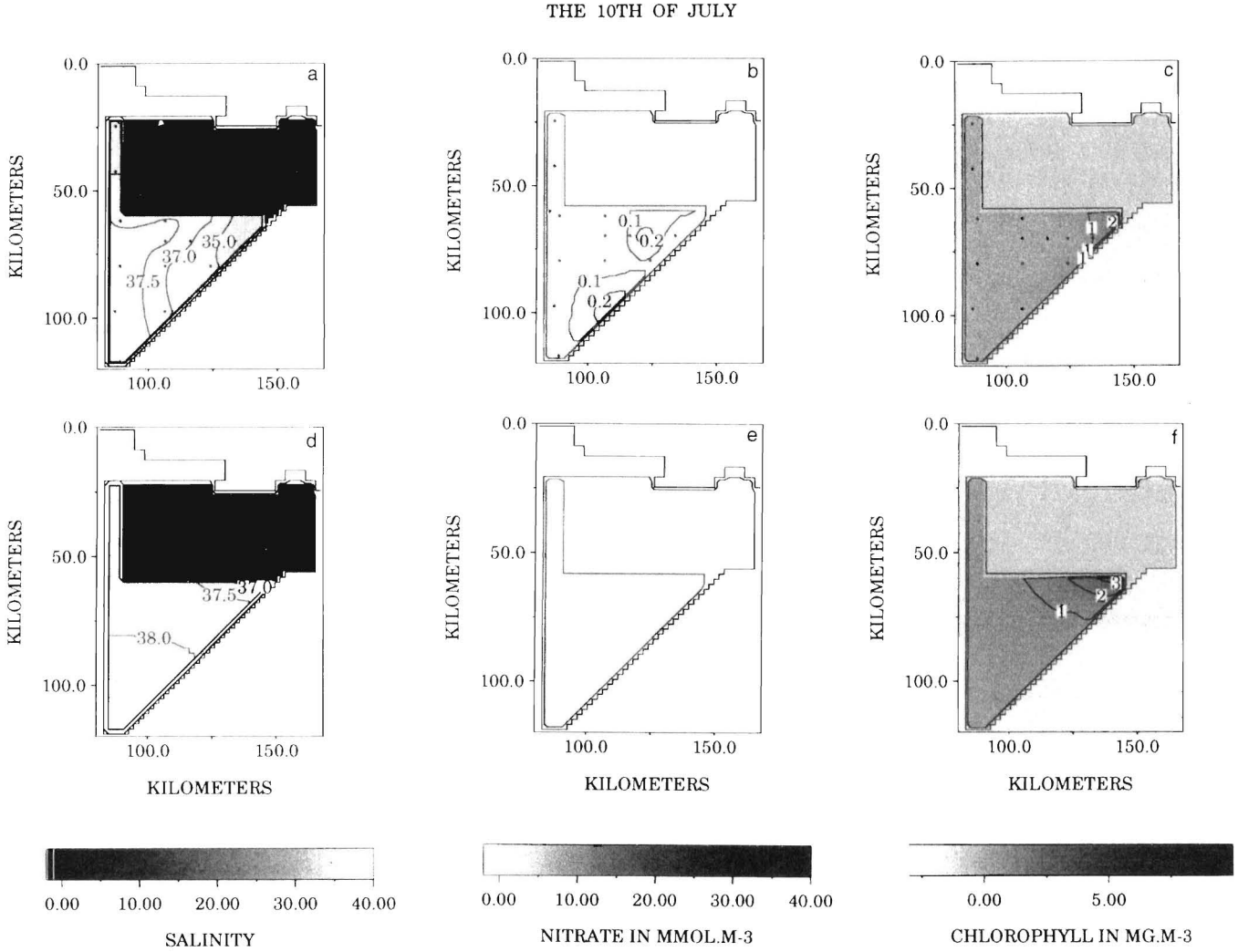

Figure 10. Comparative diagram of respectively measured salinity (a), nitrate (b), chlorophyll (c) and computed salinity (d), nitrate (e), chlorophyll (f), on the 10th July 1983.

the southwestern wind induced an eastwards extension of the plume.

Third, on the 8th of July, surface computed salinity, nitrate and chlorophyll concentrations presented a similar plume extended both south- and westwards along the coast. The chlorophyll plume extension was larger than the plume extensions of salinity and nitrate, because the phytoplankton biomass grew around the freshwater plume, which is consistent with other observations (CHEN *et al.*, 1997; LEFÈVRE *et al.*, 1997). This computed chlorophyll plume shape had the same characteristics than the observations from the CZCS and AVHRR remote sensing pictures.

Finally, our results showed three typical patterns of the plume: southwestwards associated with northwestern wind; pushed close to the coast associated with southeastern wind; semicircular (south- and westwards orientations) associated with western wind. These results confirmed the typology previously established by DEMARCQ (1985) from remote sensing pictures analysis. This typology was constituted by four typical plume shapes: the soutwestwards orientation induced by a northwestern wind observed on 60% of his pictures (Figure 11a); the plume against the coast induced by a southeastern wind on 12% of the pictures (Figure 11b); the southeastwards orientation induced by western wind on 10% of the pictures (Figure 11c); and a semicircular plume promoted by weak winds on 18% of the pictures (Figure 11d).

The results of the simulation of the EURHOGLI campaign showed that the model was able to reproduce the high variability of the Rhône river plume position under variable observed wind conditions, quite representatives of the local typical wind regime. In addition, our model confirmed that the high variability of the plume was characteristic of low Rhône river inflows, according to previous analyses performed from remote sensing pictures. Nevertheless, the present model reproduces insufficiently the offshore extension of plumes that could be explained by an offshore underestimation of the

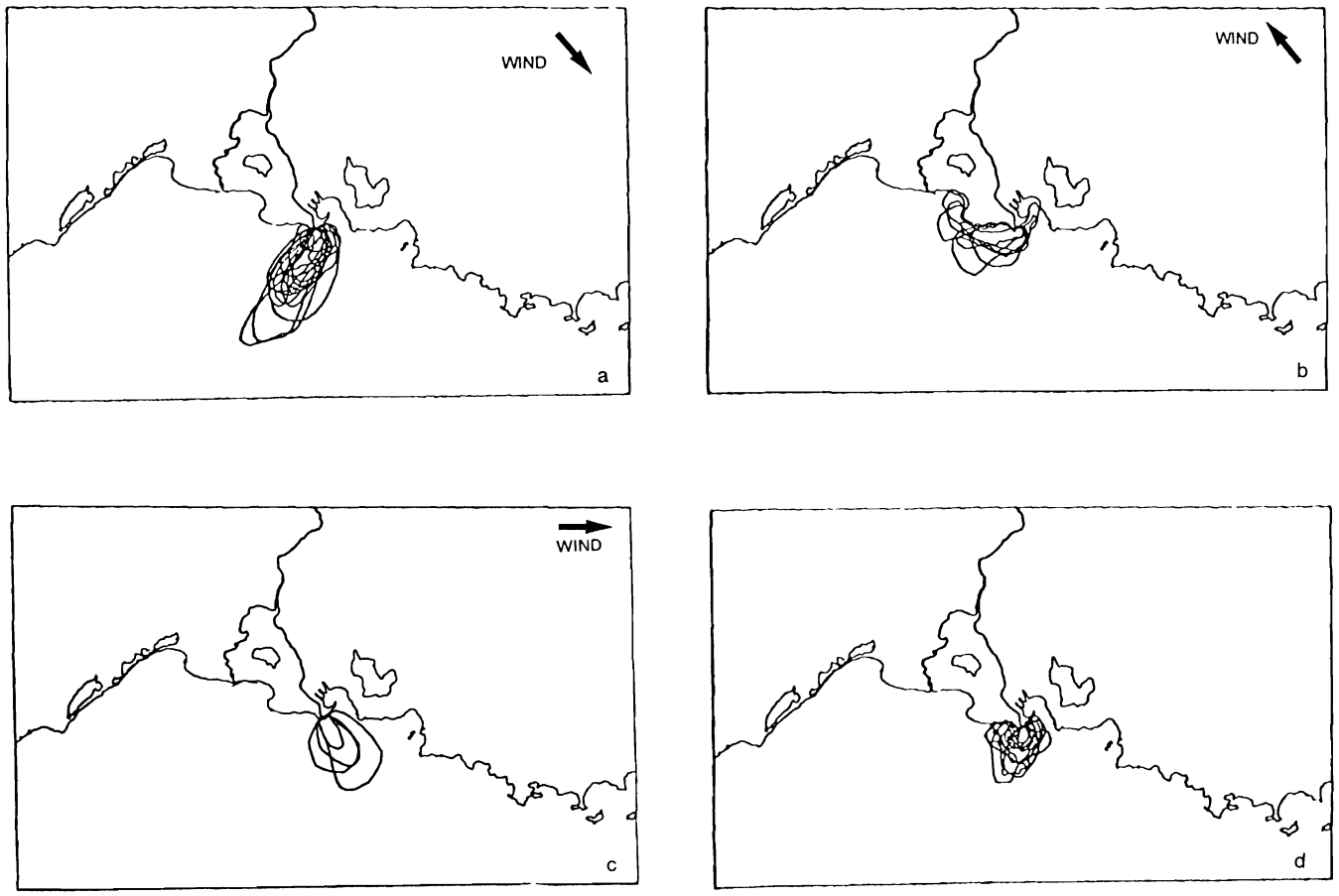

Figure 11. Typology of the Rhône river plume shape, established by Demarcq (1985) from remote sensing pictures analyses, for northwestern (a), southeastern (b), western (c) and weak (d) winds.

wind. Indeed, HSU (1986) showed that land-based wind speeds were lower than offshore wind speeds, the ratio U_{sea}/U_{land} being about 1.2. Recently KOURAFOULOU et al. (1996) used a ratio U_{sea}/U_{land} of 1.6 to simulate the river discharge on the Southeast U.S. continental shelf. In our case, the lack of offshore wind measurements did not allow to correct the land-based wind data.

Validation of Concentrations According to Freshwater Impact

The daily average computed salinity and nitrate concentrations appeared to be underestimated related to measured data. Concerning chlorophyll, computed concentrations appeared in reasonable agreement with the observations, but the computed plume shape was wider than the observed one, because of the asynchronous interpolation of field data. Indeed, the study emphasized that measurements were too spaced to give a suitable representation of the spatial structures and the temporal dynamics of the Rhône river plume. The remote sensing pictures give reliable qualitative information about the chlorophyll concentrations at large space scale, whereas measurements need to be considered at limited space scales to keep a time-space consistency. But in the future, the new sensors of the sea color like SeaWiFs, Meris or Polder will give quantitatives information about chlorophyll concentrations, and allow a new significant step in the validation of models.

On the 8th of July, nitrate concentrations decreasing (Figure 7b) might be explained by a plankton consumption that lead to reach moderate biomasses of about 5.0 $mg \cdot m^{-3}$. This value represented a level of biomass typically induced by Rhône river nutrient supply, while previous both experimental (COSTE and MINAS, 1967) and numerical (PINAZO *et al.*, 1996a and b) studies, showed that the wind alone induced, in optimal upwelling conditions, a level of biomass limited to 3.0 $mg \cdot m^{-3}$. In addition, the maximum chlorophyll concentration computed by the model on the 8th of July was located eastward in the Gulf of Fos (Figure 8f), where the water was quickly stabilized, and nitrates were accumulated, during the previous southwestern wind. Generally, it should be noted that in the case of nutrient river input at the surface layer, the wind direction seemed not to be very significant, and the less the wind intensity is, the more the production of biomass is.

In conclusion, the nutrient dynamics reproduced in the model was consistent with the previous observations of COSTE (1974) and EL SAYED *et al.* (1994), which showed that the observed Rhône river nutrient input could reach values of 50 times higher than in the case of upwelled input. The model, performed with representative forcing conditions, allowed the first attempt to quantify the frame of optimal environmental conditions for phytoplankton production in the Gulf of Lions.

LITERATURE CITED

ALBEROLA, C.; MILLOT, C., and FONT, J., 1995. On the seasonal and mesoscale variabilities of the Northern Current during the PRIMO-0 experiment in the western Mediterranean Sea. *Oceanologica Acta,*18, 163–192.

ANDERSEN, V.; NIVAL, P., and HARRIS, P., 1987. Modelling of a planktonic ecosystem in an enclosed water column. *Journal of the Marine Biological Association UK,* 67, 407–430.

ANDERSEN, V. and NIVAL, P., 1988. A pelagic ecosystem model simulating production and sedimentation of biogenic particles; role of salps and copepods. *Marine Ecology-Progress Series,* 44, 37–50.

ARAKAWA, A. and SUAREZ, M.J., 1983. Vertical differencing of the primitive equations in sigma coordinates. *Monthly Weather Review,* 111, 34–35.

ASCENCIO, E.; BORDREUIL, C.; FRASSE, M.; ORIEUX, A., and ROUX, D., 1977. Une approche des conditions météorologiques sur le golfe du Lion. *Annales de l'Institut Océanographique de Paris,* 53, 155–169.

ASSELIN, R., 1972. Frequency filters for time integrations. *Monthly Weather Review,* 100, 487–490.

BECKERS, J.M., 1991. Application of the GHER 3D general circulation model to the western Mediterranean. *Journal of Marine Systems,* 1, 315–332.

BIENFANG, P.K., 1982. Phytoplankton sinking-rate dynamics in enclosed experimental ecosystems. *In:* GRICE, G.D., and REEVE, M.R. (ed.), *Marine mesocosm; biological and chemical research in experimental ecosystems.* Springer-Verlag, New York, pp. 261–274.

BLUMBERG, A.F. and MELLOR, G.L., 1987. A description of a three dimensional coastal circulation model. *In:* HEAPS, N.S. (ed), *Three dimensional coastal ocean model.* American Geophysical Union, Washington DC, pp. 1–16.

CANIAUX, G.; ROQUET, H., and PLANTON, S., 1993. A 3-D mesoscale simulation of the ocean using data from the Athena 88 field experiment. *Journal of Marine Systems,* 4, 197–216.

CAPERON, J. and MEYER, J., 1972a. Nitrogen-limited growth of marine phytoplankton; changes in population characteristics with steady-state growth rate. *Deep Sea Research,* 19A, 601–618.

CAPERON, J. and MEYER, J., 1972b. Nitrogen-limited growth of marine phytoplankton; uptake kinetics and their role in nutrient-limited growth of phytoplankton. *Deep Sea Research,*19A, 619–632.

CHEN, C.; WIESENBURG, D.A., and XIE, L., 1997. Influences of river discharge on biological production in the inner shelf: A coupled biological and physical model of the Louisiana-Texas Shelf. *Journal of Marine Research,* 55,293–320.

CIVITARESE, G.; CRISE, A.; CRISPI, G., and MOSETTI, R., 1996. Circulation effects on nitrogen dynamics in the Ionian Sea. *Oceanologica Acta,* 19, 6, 609–622

CLOERN, J.E., 1991. Tidal stirring and phytoplankton bloom dynamics in an estuary. *Journal of Marine Research,* 49, 203–221.

CONAN, P. and MILLOT, C., 1995. Variability of the northern current off Marseille, western Mediterranean Sea, from February to June 1992. *Oceanologica Acta,* 18,193–205.

COSTE, B., 1974. Rôle des apports nutritifs minéraux rhôdaniens sur la production organique des eaux du Golfe du Lion. *Thetys,* 6, 727–740.

COSTE, B. and MINAS, H.J., 1967. Premières observations sur la distribution des taux de productivité et des concentrations en sels nutritifs des eaux de surface du Golfe du Lion. *Cahiers Océanographiques,*19, 417–429.

DEMARCQ, H., 1985. Applications de la télédétection infra-rouge et visible en océanographie; Etude de la zone Rhôdanienne, observations des zones de production dans le Golfe du Lion et estimation de l'éclairement solaire global en Méditerranée occidentale. *Thèse Doctorat,* Université Aix-Marseille 2, 226 p.

DEMARCQ, H. and WALD, L., 1984. La dynamique superficielle du panache du Rhône d'après l'imagerie infrarouge satellitaire. *Oceanologica Acta,* 7, 159–162.

DONEY, S.C.; GLOVER, D.M., and NAJJAR, R.G., 1996. A new coupled, one-dimensional biological-physical model for the upper ocean: application to the JGOFS Bermuda Atlantic Time-series Study (BATS) site. *Deep Sea Research II,* 43, 591–624.

DRUET, C. and ZIELINSKI, A., 1994. Modelling the fine structure of the phytoplankton concentration in a stably stratified sea. *Oceanologica Acta,* 17, 79–88.

EL SAYED, M.A.; AMINOT, A., and KEROUEL, R., 1994. Nutrients and trace metals in the northwestern Mediterranean under coastal upwelling conditions. *Continental Shelf Research,* 14, 507–530.

EPPLEY, R.W., 1972. Temperature and phytoplankton growth in the sea. *Fishery Bulletin,* 70, 1063–1085.

FASHAM, M.J.R., 1995. Variation in the seasonal cycle of biological production in subarctic oceans: A model sensitivity analysis. *Deep Sea Research I,* 42,1111–1149.

FENNEL, W. and NEUMANN, T., 1996. The mesoscale variability of nutrients and plankton as seen in a coupled model. *German Journal of Hydrography,* 48,1, 49–71.

FREIJE, H., 1985. Etude de la production primaire en période estivale dans le Golfe du Lion. *Thèse Doctorat,* Université Aix-Marseille 2, 125 p.

GASPAR, P.; GREGORIS, Y., and LEFEVRE, J.M., 1990. A simple eddy kinetic energy model for simulations of the oceanic vertical mixing, tests at station Papa and long-term upper ocean study site. *Journal of Geophysical Research,* 95, 179–193.

HSU, S.A., 1986. Correction of land-based wind data for offshore applications, a further evaluation. *Journal of Physical Oceanography,* 16, 390–394.

JOHNS, B. and ALI, M.A., 1990. The numerical modelling of storms surges in the Bay of Bengal. *Quarterly Journal of the Royal Meteorological Society,* 106, 1–18.

JOHNS, B.; RAO, G.S.; DUBE, S.K., and SINHA, P.C., 1991. An application of a wind-driven coastal upwelling model in the western Bay of Bengal. *Continental Shelf Research,* 11, 295–319.

KOURAFOULOU, V.H.; LEE, T.N.; OEY, L.Y., and WANG, J.D., 1996. The fate of river discharge on the continental shelf; transport of coastal low-salinity waters under realistic wind and tidal forcing. *Journal of Geophysical Research,* 101, 3435–3455.

KUHN, W. and RADACH, G. 1997. A one-dimensional physical-biological model study of the pelagic nitrogen cycling during the spring bloom in the northern North Sea (FLEX'76). *Journal of Marine Research,* 55, 687–734.

LEFEVRE, D.; WILLIAM, P.J. le B., and BENTLEY, T.L., 1995. Oxygen based production measurements in the Gulf of Lions. *Water Pollution Research Reports,* 32, 125–132.

LEFEVRE, D.; MINAS, H.J.; MINAS, M.; ROBINSON, C.; WILLIAM, P.J. le B., and WOODWARD, E.M.S., 1997. Review of gross community production and dark community respiration in the Gulf of Lions. *Deep Sea Research II,* 44, 801–832.

LOCHET, F., 1991. Transferts à l'interface continent-océan entre un système eutrophe (Rhône) et un système oligotrophe (Méditerranée nord-occidentale), importance de l'enveloppe frontale et des couches néphéloïdes. *Thèse Doctorat,* Université Aix-Marseille 2, 288 p.

MELLOR, G.L. and BLUMBERG, A.F.,1985. Modelling vertical and horizontal diffusivities and the sigma coordinate system. *Monthly Weather Review,* 113, 1379–1383.

MILLOT, C., 1990. The Gulf of Lion's hydrodynamics. *Continental Shelf Research,* 10, 885–894.

MILLOT, C. and CREPON, M., 1981. Inertial oscillations on the continental shelf of the Gulf of Lions, observations and theory. *Journal of Physical Oceanography,*11, 639–657.

MINAS, M. and MINAS, H.J., 1990. Oxygen as primary indicator in the Rhone River dilution area and the remainder of the Gulf of

Lions, with special reference to the « shallow oxygen maximum » (SOM). *Water Pollution Research Reports*, 20, 131–144.

MINAS, M. and MINAS, H.J.,1992 b. Hydrological and chemical conditions in the Gulf of Lions and relationships to primary production encountered during Cybele (first leg, 12–19 April 1990). *In: Eros 2000,* MARTIN, J.M. and BARTH, H. (eds.), *Water Pollution Research Reports*, 28, 127–138.

ORLANSKI, J., 1976. A simple boundary condition for unbounded hyperbolic flows. *Journal of Computational Physics*, 21, 255–261.

PETERSON, D.H. and FESTA, J.F., 1984. Numerical simulation of phytoplankton productivity in partially mixed estuaries. *Estuarine, Coastal and Shelf Sciences*, 19, 563–589.

PINAZO, C.; MARSALEIX, P.; MILLET, B.; ESTOURNEL, C., and VEHIL, R., 1996a. Spatial and temporal variability of phytoplankton biomass in upwelling areas of the northwestern Mediterranean, a coupled physical and biogeochemical modelling approach. *Journal of Marine Systems*, 7, 161–191.

PINAZO, C.; MARSALEIX, P.; MILLET, B.; and ESTOURNEL, C., 1996b. Réponse du phytoplancton à un forçage de vent variable en intensité et en durée, modélisation numérique des zones d'upwelling du golfe du Lion. *Comptes Rendus de l'Académie des Sciences*, série III, 319, 639–646.

QUENEY, P., 1974. *Eléments de Météorologie.* Masson, Paris.

SKOGEN, M.D.; SVENDSEN, E., and BERNTSEN, J., 1995. Modelling the primary production in the North Sea using a coupled 3D physical-chemical-biological ocean model. *Estuarine, Coastal and Shelf Sciences*, 41, 545–565.

SOTO, Y.; BIANCHI, M.; MARTINEZ, J., and REGO, J.V., 1993. Seasonnal evolution of microplanktonic communities in the estuarine front ecosystem of the Rhône river plume (northwestern Mediterranean sea). *Estuarine, Coastal and Shelf Sciences,* 37, 1–13.

STEELE, J.H., 1962. Environmental control of photosynthesis in the sea. *Limnology and Oceanography,* 7, 137–150.

TETT, P., 1987. Modelling the growth and distribution of marine microplankton. *Soc. Gen. Microbiol. Symp.*, 41, 387–425.

TETT, P., 1990a. A three layer vertical and microbiological processes model for shelf seas. Proudman Oceanograpgic Laboratory, *Report 14,* NERC.

TETT, P., 1990b. The photic zone. *In:* HERRING, P.J.; CAMBELL, A.K.; WHITFIELD, M., and MADDOCK, L. (eds.), *Light and Life in the Sea.* Cambridge University, pp. 59–87.

TUSSEAU-VUILLEMIN, M.H.; MORTIER, L., and HERBAUT, C., 1998. Modeling nitrate fluxes in an open coastal environment (Gulf of Lions). Transport versus biogeochemical processes. *Journal of Geophysical Research,* 103, C4, 7693–7708.

VAN DEN BERG, A.J.; RIDDERINKHOF, H.; RIEGMAN, R.; RUARDIJ, P.,and LENHART, H., 1996. Influence of variability in water transport on phytoplankton biomass and composition in the southern North Sea: a modelling approach (FYFY). *Continental Shelf Research,* 16, 7, 907–931.

WU, J., 1980. Wind-stress coefficients over sea surface near neutral conditions, a revisit. *Journal Physical Oceanography,* 10, 727–740.

WU, J., 1992a. Variation of the heat transfert coefficient with environmental parameters. *Journal Physical Oceanography,* 22, 293–300.

WU, J., 1992b. On moisture flux across the sea surface. *Boundary Layer Meteorology,* 60, 361–374.